Available online at www.sciencedirect.com
SCIENCE DIRECT®
International Journal of Heat and Mass Transfer 48 (2005) 4028–4040
International Journal of HEAT and MASS TRANSFER
www.elsevier.com/locate/ijhmt

Design of thermoelectric heat pump unit for active building envelope systems

Ritesh A. Khire [a], Achille Messac [a,*], Steven Van Dessel [b]

[a] Department of Mechanical and Aerospace Engineering, Rensselaer Polytechnic Institute, Troy, NY 12180, United States
[b] School of Architecture, Rensselaer Polytechnic Institute, Troy, NY 12180, United States

Received 25 June 2004; received in revised form 1 April 2005

Abstract

Active building envelope (ABE) systems represent a new thermal control technology that actively uses solar energy to compensate for passive heat losses or gains in building envelopes or other enclosures. This paper introduces initial steps in exposing the community to this new technology, and explores an optimization based design strategy for its feasible application. We discuss the overall ABE system, and focus on the design and analysis of a key component—the thermoelectric heat pump unit, or the TE unit. This unit becomes an integral part of the generic enclosure, and is a collection of thermoelectric coolers, or heaters. As a critical component of the optimization based design strategy, computationally inexpensive approximate analytical models of generic TE coolers/heaters (referred to as TE coolers) are developed. A multi-objective optimization technique is implemented to design and evaluate different design configurations of the TE unit. The multi-objective optimization simultaneously minimizes two design objectives: (1) the total input power required to operate the TE unit and (2) the number of TE coolers for economic considerations. Preliminary results indicate that the total input power required to operate the TE unit decreases as the distribution density of the TE coolers increases. In addition, the thermal resistance of the heat sink (attached to the TE cooler) plays a key role in determining the number of TE coolers required. These preliminary findings may have practical implications, influencing the implementation of the ABE system.

Keywords: Active building envelope; Thermoelectric; Optimization; Heat sink; Air conditioning; Housing

1. Introduction

Active building envelope (ABE) systems represent a new thermal control technology that actively uses solar energy to compensate for passive heat losses or gains in building envelopes or other enclosures. In ABE systems, solar radiation energy is converted into electrical energy by means of a photovoltaic unit (PV unit). Subsequently, this electrical energy is used to power a thermoelectric heat pump unit (TE unit), which is a collection of thermoelectric coolers (heaters in winter). The TE unit allows the transport of heat through the ABE wall. The PV and TE units are integrated within the ABE system enclosure. The TE unit can operate in a heating or a cooling mode, depending on the direction of the current supplied by the PV unit. This feature allows for the ABE system to be used for heating as

* Corresponding author. Tel.: +1 518 276 8145; fax: +1 518 276 6025.
E-mail address: messac@rpi.edu (A. Messac).

0017-9310/$ - see front matter © 2005 Elsevier Ltd. All rights reserved.
doi:10.1016/j.ijheatmasstransfer.2005.04.028

Nomenclature

h	natural convection coefficient
k	thermal conductivity of the thermoelectric element
k_{hs}	thermal conductivity of the heat sink
m_{hs}	mass of the heat sink
n	number of thermocouples per TE cooler
n_f	number of fins
t_f	thickness of the fin
t_b	thickness of the heat sink base plate
t_{ABE}	the thickness of the ABE wall
w_1, w_2	weights of the aggregate objective function
A	area of cross-section of the thermoelectric element
A_{ABE}	surface area of the ABE wall
A_b	area of the heat sink base plate
A_f	cross-sectional area of the fin
A_{sc}	area of the heat source in contact with the heat sink
COP	coefficient of performance
I	input current supplied by the PV unit
I_{max}	maximum allowable input current
K	thermal conductance of the thermocouple
L	length of the thermoelectric element
L_{cf}	corrected length of the fin
L_f	length of the fin
N	number of thermoelectric coolers
P_f	perimeter of the fin
P_{in}	input power supplied by the PV unit
Q_{hs}	heat dissipated through the heat sink
Q_{load}	heat dissipated by the heat source
Q_{pc}	heat absorbed at the cold end of the TE cooler
Q_{ph}	heat generated at the hot end of the TE cooler
R	electrical resistance of the thermocouple
R_b	base spreading resistance
R_f	thermal resistance of the fins
R_{hs}	thermal resistance of the heat sink
R_{th}^{TE}	thermal resistance of the TE unit
S	relative Seebeck coefficient
T_c	temperature of the cold end of the TE cooler
T_h	temperature of the hot end of the TE cooler
T_{max}	maximum allowable temperature for the TE cooler
T_o	ambient air temperature
V	input voltage supplied by the PV unit
V_{max}	maximum allowable input voltage for the TE cooler
V_s	Seebeck voltage
W_f	width of the fin

Greek symbols

ρ	electrical resistivity of thermoelectric element
ρ_{hs}	density of the heat sink
λ	ratio of the area of cross-section to the length of thermoelectric element

well as cooling applications. Among the key differences between ABE systems and conventional thermal control technologies are that the former: (i) are intended to operate using solar energy [1], (ii) are made of solid-state devices and operate silently with no moving parts, (iii) use little or no fossil energy sources, and (iv) should result in important long-term environmental benefits.

Active building envelopes: A brief description of the proposed ABE system is provided here (see Fig. 1). For more details, see [1]. The ABE system is comprised of two basic components: a photovoltaic unit (PV unit) and a thermoelectric heat pump unit (TE unit). The PV unit consists of photovoltaic cells, which are solid-state devices that convert solar radiation energy into electrical energy. The TE unit consists of thermoelectric heaters/coolers (referred to here onwards as TE coolers), which are solid-state devices that convert electrical energy into thermal energy, or the reverse. The PV and the TE units are integrated within the overall ABE enclosure. As shown in Fig. 1, the PV unit forms an envelope surrounding the external wall such that a gap is maintained between the wall and the PV unit. This gap acts as an external heat dissipation zone for the TE unit. The external walls of the proposed ABE system consist of two layers, as shown in Fig. 1. The external layer (facing the PV unit) is made of a thermal insulating material, and the internal layer is made of a material with high heat storage capacity.

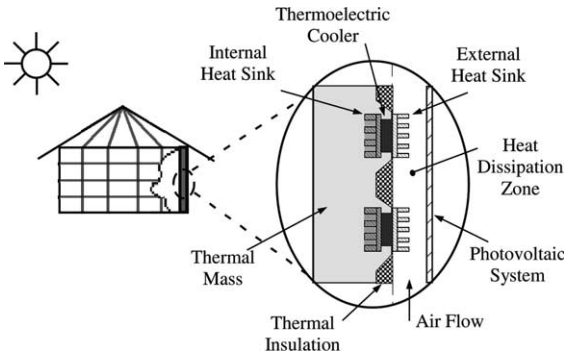

Fig. 1. Active building envelope (ABE) system.

In Fig. 1, the words "Thermal insulation" and "Thermal Mass" pertain to the external and the internal layers of the ABE wall, respectively. The TE coolers are dispersed inside the openings that are provided in the insulating layer. Each TE cooler consists of two heat sinks. As shown in Fig. 1, the internal heat sink either absorbs or dissipates heat to the thermal mass layer. The external heat sink either absorbs heat from, or dissipates heat to, the surrounding air; through natural or forced convection. In the present study, we have neglected the effect of the internal heat sink in keeping with the scope of this preliminary study.

This paper is organized as follows. Section 2 describes the approximate analytical models that are judiciously integrated in this study. Section 3 estimates the cooling load for a generic enclosure. Section 4 presents the optimization problem formulation for the design of the TE unit. The results are discussed in Section 5. Concluding remarks are provided in Section 6.

2. Basic models for ABE system

In the process of analyzing the overall ABE system, we first focus our attention on each unit in detail. In this paper, we present the design and analysis of the TE unit for the ABE system. Specifically, this section develops a computationally inexpensive model of the TE unit. Here, the individual models of the components of the TE unit are coupled, yielding a single integrated model that takes into account the effect of the heat sink on the TE cooler.

2.1. Thermoelectric cooler

This subsection describes the approximate analytical model of a TE cooler. As shown in Fig. 2, when current flows through the junction of two dissimilar conductors (also called a thermocouple), heat is either dissipated or absorbed (depending on the direction of the current) at that junction. This phenomenon is known as the Peltier effect, and causes a decrease in the temperature at the heat-absorbing junction, and a simultaneous increase in the temperature at the heat-releasing junction [2–4]. When current flows through a TE cooler that contains n thermocouples, the amount of heat absorbed at the cold junction (Q_{pc}) is given by [5,6]

$$Q_{pc} = n\left[SIT_c - K(T_h - T_c) - \frac{1}{2}I^2R\right] \tag{1}$$

where

$$K = \frac{k_1A_1}{L_1} + \frac{k_2A_2}{L_2} \tag{2}$$

$$R = \frac{\rho_1L_1}{A_1} + \frac{\rho_2L_2}{A_2} \tag{3}$$

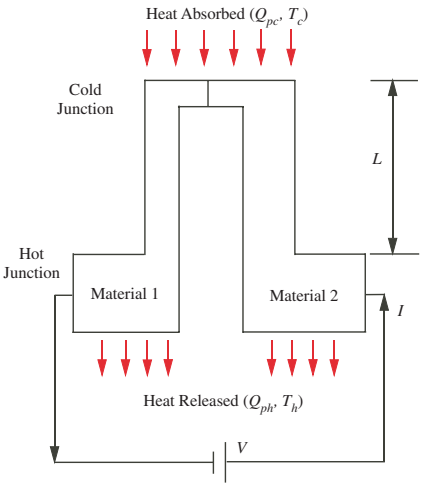

Fig. 2. Schematic of a thermocouple.

In Eqs. (1)–(3), S is the relative Seebeck coefficient of the thermocouple; I is the input current flowing through the circuit; T_c and T_h are the temperatures of the cold and the hot junctions, respectively; K is the thermal conductance of the thermocouple; R is the electrical resistance of the thermocouple; k is the thermal conductivity; ρ is the electrical resistivity; and A and L represent the cross-sectional area and the length of the thermoelectric element, respectively. The subscripts 1 and 2 refer to the thermoelectric materials 1 and 2, respectively.

2.2. Heat sink

Heat sinks lower or maintain the temperature of a device by dissipating heat into the surrounding medium. The primary requirement of an effective heat sink is to provide a low thermal resistance path for heat dissipation. In ABE systems, heat sinks are required to dissipate the heat generated at the hot side of the TE coolers. The performance characteristics of the TE cooler (e.g., input power, heat absorption capacity) are greatly affected by the thermal resistance of the associated heat sink. Failure to dissipate the required heat from the TE cooler may result in an increase in its hot side temperature. As per Holman [7], the heat dissipated by a heat sink is given by

$$Q_{hs} = \frac{T_h - T_o}{R_{hs}} \tag{4}$$

where Q_{hs} is the heat dissipated by the heat sink, T_h is the temperature of the heat source (in the ABE systems, the hot end of the TE cooler), T_o is the ambient air temperature, and R_{hs} is the thermal resistance of the heat sink, given by

$$R_{hs} = R_f + R_b \tag{5}$$

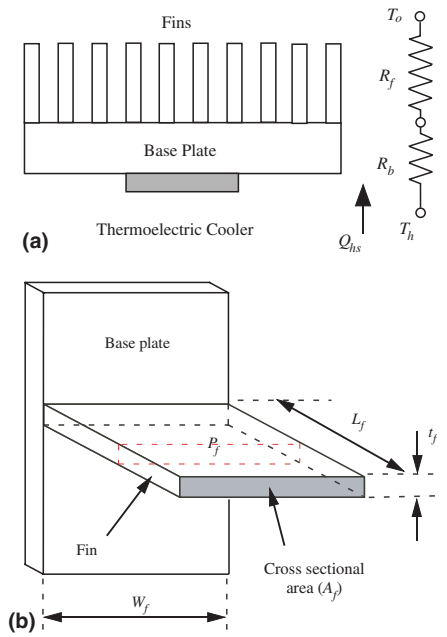

Fig. 3. Schematic of a heat sink: (a) thermal circuit of a heat sink and (b) geometric parameters of a fin.

where R_f and R_b represent the thermal resistances of the fins and the base (also called the base spreading resistance), respectively. Fig. 3(a) shows the thermal circuit of a heat sink. As shown in Fig. 3(a), the fin resistance and the base spreading resistance are in series. The heat generated by the heat source (the hot side of the TE cooler) is conducted through the heat sink, which is then dissipated to the surrounding medium by convection. The following subsections present the approximate analytical models for estimating the fin resistance and the base spreading resistance of the heat sink.

2.2.1. Fin resistance

A typical heat sink consists of thin metal projections, called fins, as shown in Fig. 3(a). Fins provide additional surface area to increase the convection heat transfer. When a heat sink is exposed to natural convection, it is called a passive heat sink, and when it is exposed to forced convection, it is called an active heat sink [7]. In the present study, we analyze a passive heat sink. Also, for the present study, we will consider an extrusion type heat sink, which is suitable for low heat dissipation applications such as ABE systems. The thermal resistance of a single fin heat sink is given by [7]

$$R_f = \frac{1}{\sqrt{hP_f k_{hs} A_f}\tanh(mL_{cf})} \tag{6}$$

where

$$m = \sqrt{\frac{hP_f}{k_{hs}A_f}} \tag{7}$$

In Eqs. (6) and (7), h is the natural convection coefficient; k_{hs} is the thermal conductivity of the heat sink; and P_f, A_f, and L_{cf} are the perimeter, the area of cross-section, and the corrected length of the fin, respectively. These quantities are evaluated as [7]

$$P_f = 2(W_f + t_f) \tag{8}$$

$$A_f = W_f \times t_f \tag{9}$$

$$L_{cf} = L_f + t_f/2 \tag{10}$$

In Eqs. (8)–(10), the variables W_f, t_f, and L_f represent the width, the thickness, and the length of the fin, respectively. The basic geometric parameters of a fin are illustrated in Fig. 3(b). By multiplying Eq. (6) by the number of fins (n_f), we can estimate the fin resistance of a multiple fin heat sink.

We note that, in this paper, we approximate the heat transfer between the fin surfaces and the surrounding air using the natural convection coefficient (h). This approximation assumes that the air in contact with the fin surfaces is maintained at the ambient air temperature (T_o), at all times. Such an approximation is in agreement with the preliminary nature of this design study. However, in future studies, a detailed analysis of the heat transfer process at the fin surfaces is required, which takes into account the effect of the localized increase in the air temperature on the natural convection process.

2.2.2. Base spreading resistance

The base spreading resistance needs to be considered when a heat source with a smaller heat dissipation area is mounted over a heat sink with a larger base plate area [8], as shown in Fig. 3(a). This increases the base plate temperature at the location of the heat source. The base spreading resistance is given by the empirical formula [8]

$$R_b = \left[\frac{\sqrt{A_b} - \sqrt{A_{sc}}}{k_{hs}\sqrt{\pi A_b A_{sc}}}\right]\left[\frac{\lambda_b k_{hs} A_b R_{avg} + \tanh(\lambda_b t_f)}{1 + \lambda_b k_{hs} A_b R_{avg}\tanh(\lambda_b t_f)}\right] \tag{11}$$

where

$$\lambda_b = \frac{\pi^{3/2}}{\sqrt{A_b}} + \frac{1}{\sqrt{A_{sc}}} \tag{12}$$

In Eqs. (11) and (12), A_b is the area of the base plate of the heat sink; A_{sc} is the area of the heat source, which is in contact with the base plate; and R_{avg} is the average thermal resistance of the heat sink, which is assumed to be equal to the fin resistance, R_f, according to Ref. [9]. In the current paper, we assume the spacing between fins to be equal to the fin thickness. The area of the heat sink base plate is determined as $A_b = (2n_f - 1)t_f w_f$.

2.3. Estimating the effect of heat sink on TE cooler

As stated in the previous subsection, a heat sink is required to dissipate the heat generated at the hot junction

of the TE cooler. The heat generated at the hot junction of the TE cooler (Q_{ph}) is given by [10]

$$Q_{ph} = Q_{pc} + VI \tag{13}$$

where V is the voltage across the TE unit. Since the heat sink is required to dissipate this heat, we have $Q_{hs} = Q_{ph}$. Using Eqs. (4) and (13), we obtain an expression for the temperature at the hot end of the TE cooler as [10]

$$T_h = T_o + (Q_{pc} + VI)R_{hs} \tag{14}$$

Substituting Eq. (14) into Eq. (1) to eliminate T_h, we can determine the effect of a heat sink on a TE cooler; namely, the dependence of Q_{pc} on R_{hs}.

We conclude this section by commenting on the model accuracy assessment work that we have performed. We have assessed the accuracies of the approximate analytical models described in this section by comparing their results with those from more comprehensive models developed in the literature, which would be less suitable for the preliminary nature of our optimization based design study. We used the model developed by Visser and de Kock [11] to assess the accuracy of the heat sink model, and the model developed by Nagy and Buist [10] to assess the accuracy of the model for estimating the effect of the heat sink on the TE cooler [12]. We observed that the difference between the results from the two models (approximate and comprehensive) is less than 15%, which is acceptable for this study. These comparative results lend sufficient credence to the analytical models presented in this section, making them appropriate for the preliminary optimal design of the TE unit. Next, we evaluate different configurations of the TE unit for a generic enclosure. In the next section, a cooling load is estimated for this enclosure under certain assumed conditions.

3. Estimation of cooling load for a generic enclosure

To demonstrate the application of the proposed optimization based strategy to design the TE unit of the ABE system, we analyze the model of a 1 m × 1 m × 1 m generic enclosure. This section provides the assumptions made in this design study, and the estimation of the cooling load for this enclosure. Fig. 4 schematically represents the generic enclosure for which the TE unit is designed.

3.1. Assumptions

The following assumptions are made for the generic enclosure. (1) The thickness of the ABE wall is $t_{ABE} = 0.15$ m. (2) Only one of the four sidewalls acts as the ABE wall, and heat losses or gains from the other sidewalls are negligible. (3) The thermal conductivity of the ABE wall is $k_{ABE} = 0.05$ W/m K. (4) The external temperature is $T_o = 38$ °C, and the internal temperature is $T_i = 20$ °C. (5) The conduction heat transfer through the ABE wall is the only mode of heat transfer. (6) All TE coolers in a TE unit absorb equal amount of heat, and the total heat absorption is uniform throughout the wall. (7) Each TE cooler has heat sinks capable of absorbing and releasing the required amount of heat. (8) All the TE coolers are connected in series. (9) The temperature of the cold end of the TE cooler is equal to the internal temperature ($T_c = T_i$). (10) The effect of the change in the external temperature, T_o, on the performance of the PV unit is neglected. (11) The effect of air circulation on the overall heat transfer process is neglected.

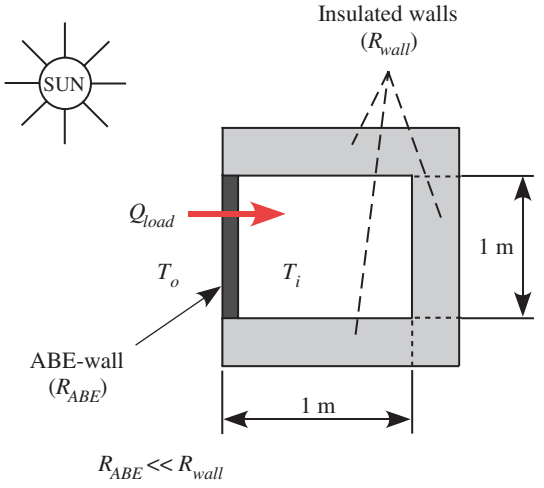

Fig. 4. Generic enclosure containing single ABE wall.

3.2. Estimation of cooling load

Fig. 4 shows the top view of the generic enclosure (1 m × 1 m × 1 m), which is used to demonstrate the application of the proposed strategy for designing a generic TE unit. We assume that the heat transfer from the external environment into the generic enclosure (or the reverse) is through the ABE wall only. The amount of heat conducted through the ABE wall is given by Fourier's law as

$$Q_{load} = k_{ABE}A_{ABE}\frac{T_o - T_i}{t_{ABE}} \tag{15}$$

where A_{ABE} is the surface area of the ABE wall. For the generic enclosure, $A_{ABE} = 1$ m × 1 m. Substituting the appropriate numerical values from Section 3.1, we obtain the heat gained by the enclosure through conduction as 6 W.

Apart from the heat gained because of conduction, a typical room with 10 m^2 floor area gains approximately

240 W of heat from the electrical appliances and the people in that room. For the generic enclosure, the floor area is 1 m^2 or 10% of the typical room described above. To account for the additional heat gained because of the factors described above, we add $0.1 \times 240 = 24$ W to the heat gain. Thus the total heat gain is $6 + 24 = 30$ W. This heat gain will act as the cooling load, Q_{load}, for the ABE system. To compensate this cooling load, we identify the optimal configurations of the TE units. The next section describes the optimization based design strategy for the TE unit.

4. Optimization based design strategy

This section describes the proposed strategy to design an appropriate configuration of the TE unit for the generic enclosure described in the previous section. This strategy involves the application of multi-objective optimization to obtain a preliminary conceptual design configuration of the TE unit. According to the previous section, the estimated total cooling load for the generic enclosure is 30 W. Using multi-objective optimization, we determine the optimal number of TE coolers and the appropriate heat sink geometry, to compensate the estimated cooling load. In this paper, we consider two design objectives: (1) electrical power required to operate the TE unit, and (2) the number of TE coolers. Both of the objectives are minimized simultaneously by combining them into a single aggregate objective function (AOF) [13]. The optimization problem involves a coupling between the performance of the TE cooler and that of the heat sink. The following subsections describe the design variables, the design constraints, and the objective function for formulating the optimization problem.

4.1. Design variables

The optimization problem involves seven design variables, two for the TE cooler and five for the heat sink. The number of TE coolers (N) and the input current (I) are the two design variables for the TE cooler. For the heat sink, the five design variables are: the length of the fin (L_f), the width of the fin (W_f), the thickness of the fin (t_f), the number of fins (n_f), and the thickness of the base plate (t_b). During the optimization process, the number of TE coolers is not allowed to become less than one; and no upper limit is provided for the number of TE coolers. The TE coolers are selected from the Melcor product catalog [14]. The input current (I) is not allowed to exceed the maximum allowable current (I_{max}), which is specified in the Melcor product catalog. The upper and the lower bounds imposed on the remaining design variables are given in the optimization problem statement (Eqs. (24)–(28)). (Note that the upper and lower bounds are in mm.)

4.2. Design constraints

The total heat absorbed by all the TE coolers is used as an equality constraint in the optimization problem. Eq. (1) determines the amount of heat absorbed by a single TE cooler (Q_{pc}). The total heat absorbed by all the TE coolers is calculated by multiplying the amount of heat absorbed by a single TE cooler by the number of TE coolers (N). During the optimization process, the total heat absorbed by all the TE coolers is constrained to equal the estimated cooling load (Q_{load}).

The temperature of the hot side of the TE cooler (T_h) is used as the first inequality constraint in the optimization problem. Eq. (14) evaluates the temperature of the hot side of the TE cooler. This temperature is not allowed to exceed the maximum allowable temperature for the TE cooler (T_{max}), which is specified in the Melcor product catalog [14].

The input voltage (V) applied to a single TE cooler is used as the second inequality constraint in the optimization problem. The input voltage for a single TE cooler is given by

$$V = S(T_h - T_c) + IR \tag{16}$$

This input voltage is not allowed to exceed the maximum voltage (V_{max}), which is specified in the Melcor product catalog [14]. For favorable numerical conditioning properties of the optimization process, all constraints are normalized as shown in Eqs. (19)–(21).

4.3. Objective functions

4.3.1. Input power

The total electrical power (P_{in}) required to operate all the TE coolers, is used as the first design objective and is given by

$$P_{in} = N \times V \times I \tag{17}$$

In ABE systems, the TE unit is powered by the PV unit (solar cells). There are several reasons why it is imperative that the input power, which is supplied by the PV unit, be minimized. The PV unit only produces electrical energy during the part of the day when solar radiation is available [15]. The surface area available to place the PV unit on the ABE wall is limited. The limited available steady state solar power may not meet peak demand. As a result, there may be a need to store power for use at night and at peak power demand periods. Hence, minimizing the input power is central to the feasibility of this system.

4.3.2. Number of TE coolers

We use the number of TE coolers (N) as the second design objective in this paper. There are several

important reasons for minimizing N. One of the most important reasons is that the cost of the ABE system will largely depend on the number of TE coolers and heat sinks used. We note that the economic viability of ABE systems will play a major role in its design process, and warrants a systematic development of the appropriate cost models. However, a detailed economic analysis is beyond the scope of this paper. Instead, we include the number of TE coolers (N) as the second design objective to account for economic considerations of ABE systems, and this design objective is also minimized.

4.4. Optimization problem statement

Our preliminary investigation shows that a trade-off exists between the two design objectives, the input power and the number of TE coolers. That is, the input power decreases as the number of TE coolers increases and vice-versa (details provided in Section 5.1). We formulate a multi-objective optimization problem to minimize these two conflicting objectives. The multi-objective optimization problem statement to design the appropriate TE unit configuration is as follows:

$$\min_{N,I,L_f,W_f,t_f,n_f,t_b} \quad w_1 P_{in} + w_2 N \tag{18}$$

subjected to

$$\frac{N Q_{pc}}{Q_{load}} - 1 = 0 \tag{19}$$

$$\frac{V}{V_{max}} - 1 \leqslant 0 \tag{20}$$

$$\frac{T_h}{T_{max}} - 1 \leqslant 0 \tag{21}$$

$$1 \leqslant N \tag{22}$$

$$0.01 \leqslant I \leqslant I_{max} \tag{23}$$

$$1 \leqslant L_f \leqslant 50 \tag{24}$$

$$1 \leqslant W_f \leqslant 50 \tag{25}$$

$$1 \leqslant t_f \leqslant 5 \tag{26}$$

$$1 \leqslant t_b \leqslant 5 \tag{27}$$

$$2 \leqslant n_f \leqslant 50 \tag{28}$$

Eq. (18) represents a weighted-sum based aggregate objective function [13] that combines the two design objectives. In Eq. (18), w_1 and w_2 represent the weights corresponding to the input power and the number of TE coolers, respectively. These weights represent the relative importance given to the two design objectives, and are selected such that $0 \leqslant w_1, w_2 \leqslant 1$ and $w_1 + w_2 = 1$. Here, $w_1 = 1$ and $w_2 = 0$ indicates that we minimize the input power alone, and $w_1 = 0$ and $w_2 = 1$ indicates that we minimize the number of TE coolers alone. The combination $w_1 = 0.5$ and $w_2 = 0.5$, for example, represents an intermediate level of compromise between the design objectives.

Table 1
TE coolers used in the TE unit design configurations

Melcor product #	λ (m)	# of thermocouples/TE cooler (n)					
		7	17	31	63	71	127
CP1.0-n-08L	5.0×10^{-4}	x	x	x	x	x	x
CP1.0-n-06L	6.1×10^{-4}	x	x	x	x	x	x
CP1.0-n-05L	7.9×10^{-4}	x	x	x	x	x	x

x: Cases evaluated in this study.

4.5. Design configurations of the TE unit

We select the "CP1.0-n-zzL" class of TE coolers manufactured by Melcor Corporation, USA, to design the TE unit. Here, n represents the number of thermocouples per TE cooler, and zz is a two digit number assigned by Melcor Corporation to represent the value of λ (the ratio of the cross-sectional area, A, to the length, L, of the thermoelectric element). The detailed specifications of this class of TE coolers are given in the Melcor product catalog [14]. Three sub-classes of the "CP1.0-n-zzL" class of TE coolers are evaluated, each having a different value of λ. Each sub-class is further divided into six different design configurations. We evaluate $6 \times 3 = 18$ different design configurations using the strategy described in the previous subsections. Table 1 shows the different TE coolers that are evaluated in this study. The three sub-classes of TE coolers are given in the first column of Table 1. The second column shows the values of λ corresponding to each sub-class mentioned in the first column. The headings of columns 3–8 represent the number of thermocouples per TE cooler. The configurations of the TE unit that are evaluated in this paper are represented by the symbol "x".

5. Results and discussion

In this section, we present the results of the design study conducted for the TE unit of the generic enclosure. The results of the present design study are shown in Fig. 5(a)–(h) and tabulated in Table 2. The detailed discussions of these results are given in the following subsections. The selection of the optimal TE unit configuration is also discussed.

5.1. Trade-off between input power and number of TE coolers

In this subsection, we discuss the trade-off characteristics between the input power and the number of TE

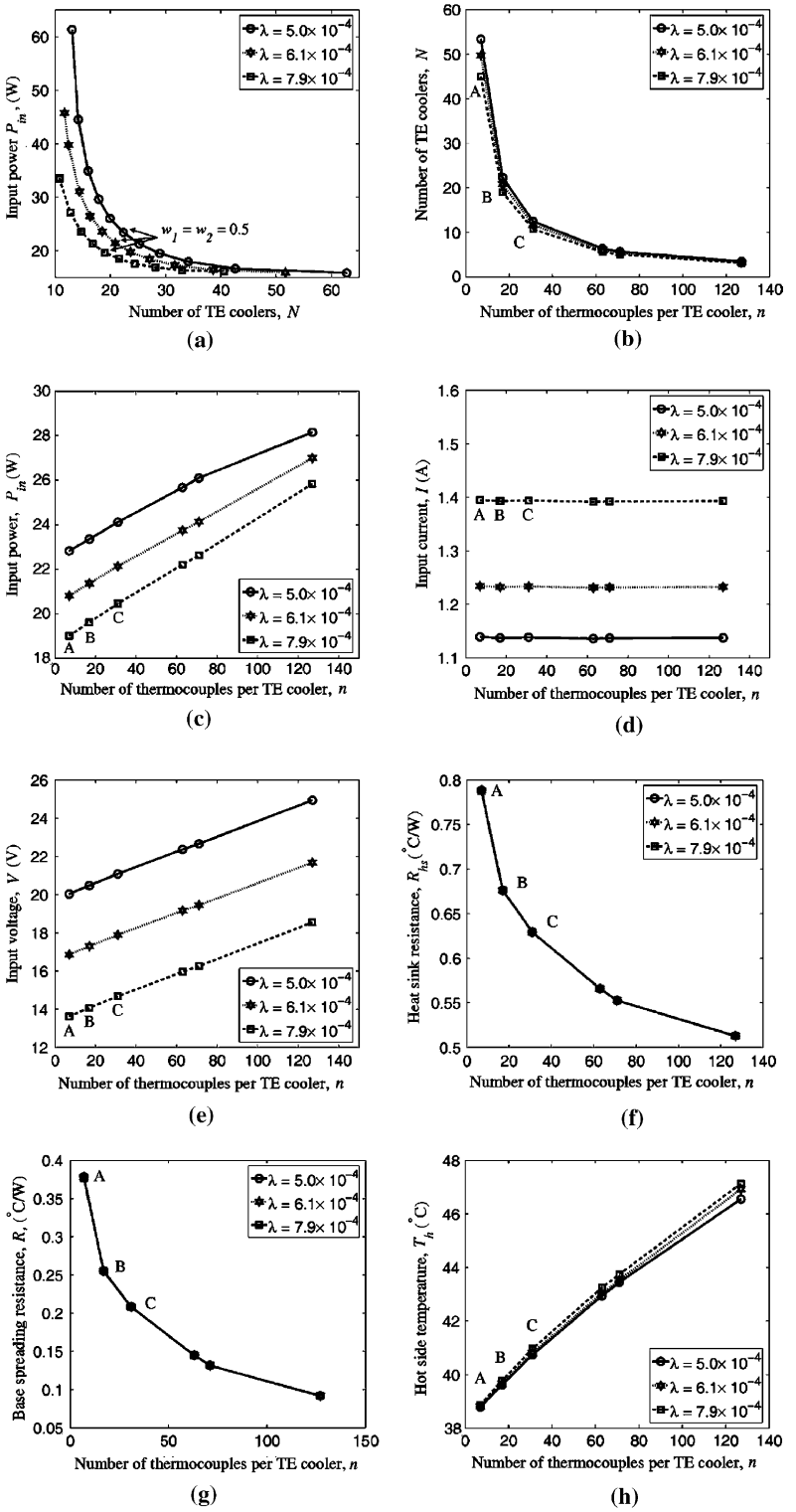

Fig. 5. Optimization results for different design configurations: (a) trade-off curves, (b) number of TE coolers, (c) total input power, (d) input current for single TE cooler, (e) total input voltage, (f) heat sink resistance, (g) base spreading resistance, and (h) hot side temperature.

Table 2
Optimal parameters for all TE unit configurations

n	7	17	31	63	71	127
CP1.0-n-08L type cooler ($\lambda = 5.0 \times 10^{-4}$ m)						
t_f	1	1	1	1	1	1
W_f	50	50	50	50	50	50
L_f	50	50	50	50	50	50
n_f	50	50	50	50	50	50
t_b	5	5	5	5	5	5
I	1.139	1.137	1.138	1.136	1.136	1.137
N	53.375	22.309	12.459	6.380	5.696	3.485
P_{in}	22.827	23.35	24.122	25.680	26.107	28.141
COP	1.314	1.284	1.243	1.168	1.149	1.066
R_{hs}	0.788	0.676	0.629	0.566	0.552	0.513
V	0.375	0.918	1.692	3.506	3.977	7.153
T_h	38.780	39.617	40.733	42.939	43.44	46.556
R_{th}^{TE}	0.0148	0.0303	0.0505	0.0887	0.0970	0.1472
CP1.0-n-06L type cooler ($\lambda = 6.2 \times 10^{-4}$ m)						
t_f	1	1	1	1	1	1
W_f	50	50	50	50	50	50
L_f	50	50	50	50	50	50
n_f	50	50	50	50	50	50
t_b	5	5	5	5	5	5
I	1.234	1.232	1.233	1.231	1.231	1.232
N	49.692	20.829	11.691	6.038	5.412	3.274
P_{in}	20.813	21.367	22.138	23.751	24.136	27.002
COP	1.441	1.404	1.355	1.263	1.242	1.111
R_{hs}	0.787	0.676	0.629	0.566	0.552	0.513
V	0.339	0.830	1.530	3.172	3.593	6.620
T_h	38.805	39.668	40.806	43.038	43.528	46.931
R_{th}^{TE}	0.0159	0.0325	0.0538	0.0937	0.1021	0.1567
CP1.0-n-05L type cooler ($\lambda = 7.9 \times 10^{-4}$ m)						
t_f	1	**1**	1	1	1	1
W_f	50	**50**	50	50	50	50
L_f	50	**50**	50	50	50	50
n_f	50	**50**	50	50	50	50
t_b	5	**5**	5	5	5	5
I	1.395	**1.393**	1.394	1.391	1.392	1.393
N	44.990	**18.989**	10.731	5.633	5.066	3.134
P_{in}	19.018	**19.610**	20.461	22.219	22.640	25.843
COP	1.577	**1.529**	1.466	1.350	1.325	1.160
R_{hs}	0.787	**0.676**	0.629	0.566	0.552	0.513
V	0.303	**0.741**	1.367	2.833	3.209	5.917
T_h	38.858	**39.767**	40.959	43.246	43.742	47.140
R_{th}^{TE}	0.0175	**0.0356**	0.0586	0.1005	0.1091	0.1637

coolers. Fig. 5(a) shows the trade-off curves for the three TE coolers that are shown in the fourth column of Table 1 (that is, TE coolers with $n = 17$). Each curve in Fig. 5(a) corresponds to the specific value of λ. To generate these trade-off curves, we change the weights w_1 and w_2 (Eq. (18)) between 0 and 1 in 10 equal increments. On each curve shown in Fig. 5(a), the point to the extreme right represents the case, where $w_1 = 1$ and $w_2 = 0$ (minimizing the input power alone). Similarly, the point to the extreme left on each curve represents the case, where $w_1 = 0$ and $w_2 = 1$ (minimizing the number of TE coolers alone). As expected, minimizing only the input power results in a large number of TE coolers (extreme right) and minimizing only the number of TE coolers results in a large input power (extreme left). However, the case $w_1 = w_2 = 0.5$ optimizes both of these design objectives simultaneously, with relatively even importance. We observed similar trade-off characteristics for all the values of n that are evaluated in this study. Based on these observations, we use $w_1 = 0.5$ and $w_2 = 0.5$ in Eq. (18) for the subsequent discussion. However, different designer preferences can be specified with

respect to the two design objectives by simply selecting an appropriate set of weights.

From Fig. 5(a), we observe that the TE cooler with $\lambda = 7.9 \times 10^{-4}$ m results in the minimum objective function values compared to the other two values of λ. We observed similar behavior for all values of n considered in this study. Hence, TE coolers with $\lambda = 7.9 \times 10^{-4}$ m ("CP1.0-*n*-05L" class) are assumed preferred over the other two classes.

In the following subsections, we discuss the effect of important parameters on the performance of the TE unit. Also, we select the number of thermocouples, n, for the "CP1.0-*n*-05L" class of TE coolers, that offers the optimal TE unit configuration. We note that in Fig. 5(b)–(h), the horizontal axis represents n.

5.2. Number of thermoelectric coolers

The number of TE coolers is one of the design objectives used in this paper. In Fig. 5(b), the x-axis shows the number of thermocouples per TE cooler (n), and the y-axis shows the number of TE coolers (N) required to compensate the estimated cooling load. As the number of thermocouples per TE cooler, n, increases, the number of TE coolers, N, required to compensate the estimated cooling load decreases. This relationship is in agreement with our expectations. However, the relation between the total number of TE coolers, N, and the number of thermocouples per TE cooler, n, is not linear. The explanation for this behavior is given in Section 5.7. From Fig. 5(b), We can also observe that the number of TE coolers is not significantly affected by the value of λ.

Although we minimize the number of TE coolers in the optimization formulation, we note that for a TE unit configuration with a small number of TE coolers (less than 10), the heat absorption across the ABE wall may not be uniform. This will violate one of the assumptions made in this study (Assumption 6 in Section 3.1). In other words, the approximate analytical model will not adequately predict the actual behavior of the TE unit for the generic enclosure.

Based on the above discussion, some of the TE coolers from the preferred "CP1.0-*n*-05L" class become less desirable, as they result in $N < 10$. In Fig. 5(b), the TE unit configurations marked A, B, and C have $N \geqslant 10$ and are expected to ensure relatively uniform heat absorption across the ABE wall. Hence, these three TE unit configurations are preferred over the other TE unit configurations. Configurations A, B, and C require approximately 45 TE coolers of CP1.0-7-05L type, 20 TE coolers of CP1.0-17-05L type, and 10 TE coolers of CP1.0-31-05L type, respectively. We will select one of these configurations as the most preferred design based on the second design objective, the input power, which is discussed next.

5.3. Total input power

The total input power is the second design objective used in this paper. Fig. 5(c) shows the total input power, P_{in}, for each of the configurations evaluated in this study. The x-axis shows the number of thermocouples per TE cooler, and the y-axis depicts the input power. As the number of thermocouples per TE cooler increases, so does the total input power. From Fig. 5(b), the number of TE coolers required to compensate the cooling load decreases as the number of thermocouples per TE cooler increases. We can then observe that as the distribution density of the TE coolers increases, the total input power required to operate the ABE system decreases, for the TE unit configurations evaluated in this study. There would reach a point where this conclusion goes beyond practical and economic implementation feasibility.

To identify the most appropriate configuration, we make the following observations. From Fig. 5(c), the TE unit configurations A, B, and C require relatively lower input power than the other configurations. Hence, these three configurations are chosen as the preferred ones, among the various TE unit configurations evaluated in this study. From Fig. 5(c), the preferred TE unit configuration A requires the lowest input power, followed by the configurations B and C, in that order.

Although the preferred configuration A requires the lowest input power among the three, it requires a large number of TE coolers (see Fig. 5(b)). An opposite behavior can be observed for the preferred configuration C. However, the configuration B offers a balance between the number of TE coolers and the input power, compared to the other two configurations. Hence, based on the two design objectives used in this paper, we select the TE unit configuration B as the most preferred design configuration. This TE unit configuration consists of 20 TE coolers of CP1.0-17-05L type, and requires approximately 19.6 W of input power (Fig. 5(c)), which needs to be supplied by the PV unit. The details of the most preferred configuration B are shown in bold letters in Table 2.

It is important to note that the results of the present study may be improved by taking into account other important practical considerations, such as the thermal capacity of the ABE wall, and the effect of air circulation on the overall heat transfer process. In the following subsections, we discuss the effect of other important parameters on the performance of the TE unit in general, and on that of configuration B in particular.

5.4. Input current

The input current required to operate a TE cooler in each configuration of the TE unit is shown in Fig. 5(d). The x-axis shows the number of thermocouples per TE

cooler, and the y-axis shows the input current. The input current decreases as the number of thermocouples per TE cooler increases. However, this decrease in the input current is less than 1%, for the range of design configurations evaluated in this study. As stated in the assumptions (Section 3.1), the TE coolers are connected in series and therefore the same current flows through all of them. Hence, every configuration of the TE unit will require the same input current as shown in Fig. 5(d). It is important to note that the relationship between the input current and the number of thermocouples per TE cooler is not perfectly linear, as is seen in Fig. 5(d). The nonlinearities in the modeling equations, and the coupling between the TE cooler and the heat sink are expected to cause this behavior. A comprehensive examination of this behavior of the input current is beyond the scope of this paper.

The TE unit configuration B requires 1.4 A of input current. The PV unit, which comprises solar cells, is expected to supply this input current. It may not be feasible for a single solar cell to produce 1.4 A of current. In such a case, multiple solar cells connected in a parallel circuit can be used to generate the required input current. We note that, in the present paper, we have not used the input current as a design objective in keeping with the scope of this study. However, the input current may assume significance, especially in the regions where ample sunlight is not available, as the current generated by the PV unit is proportional to the intensity of the incident solar radiation [15]. Next, we examine the voltage across the TE unit, which expectedly has a lesser impact on the selection process.

5.5. Input voltage across the TE unit

Fig. 5(e) shows the input voltage across the TE unit for each design configuration. The x-axis and the y-axis represent the number of thermocouples per TE cooler and the input voltage, respectively. Since TE coolers are connected in series, the input voltage across the TE unit is the product of the input voltage per TE cooler, V, (Table 2) and the number of TE coolers, N. The input voltage across the TE unit increases linearly with the number of thermocouples per TE cooler. Since the PV unit can be treated as a current source, the input voltage across the TE unit will have little impact on the selection of the TE unit configuration.

According to Eq. (16), the input voltage is the sum of two components. The first is the product of the input current, I, and the electrical resistance, R; and is therefore an explicit function of the input current. The second is the Seebeck voltage, which is given by

$$V_s = S(T_h - T_c) \tag{29}$$

According to Eq. (14), for a given heat sink resistance, R_{hs}, the hot side temperature is an implicit function of the input current. Hence, we deduce that the input voltage for the TE unit is a function of the input current, and will have little impact on the selection of the TE unit configuration. However, the input voltage across the TE unit is one of the factors for consideration in the selection of the PV unit. (Note that the design of the PV unit is not a part of the present study.) For the preferred configuration B, the total input voltage across the TE unit is 14.1 V (see Fig. 5(e)).

The input voltage per TE cooler is used as one of the constraints in the optimization problem. It is useful to note that the input voltage per TE cooler was not an active constraint for any design configuration. For all of the design configurations, the input voltage per TE cooler was always less than one-third of the maximum input voltage (V_{max}) [14]. Hence, in future analyses, which may involve combining the models of the PV unit, the inclusion of the voltage constraint may not prove critical.

5.6. Coefficient of performance

Coefficient of performance (COP) [7] is a measure of the efficiency of the TE unit and is evaluated as

$$\mathrm{COP} = \frac{\text{Heat absorbed}}{\text{Input power}} = \frac{Q_{load}}{P_{in}} \tag{30}$$

The COP values for all of the design configurations are given in Table 2. Since the same cooling load is applied to all design configurations ($Q_{load} = 30$ W), the COP is inversely proportional to the total input power, as evaluated in Section 5.3. Hence, the plot of the COP versus the number of thermocouples per TE cooler would show inverse trends compared to those in Fig. 5(c). For the preferred configuration B, the COP is 1.529 (see Table 2).

5.7. Thermal resistance of the heat sink

Here we explain how the thermal resistance of the heat sink and the total number of TE coolers decrease as the number of thermocouples per TE cooler increases. These observations represent the likely trends in the properties of optimal ABE systems.

For each configuration of the TE unit, the thermal resistance of the heat sink is shown in Fig. 5(f). The x-axis and the y-axis represent the number of thermocouples per TE cooler and the thermal resistance of the heat sink, respectively. The required thermal resistance of the heat sink decreases rapidly as the number of thermocouples per TE cooler increases. According to Fig. 5(b) (Section 5.2), the relation between the number of TE coolers and the number of thermocouples per TE cooler is also nonlinear. The various nonlinearities lead to some notable observations. As the number of thermocouples per TE cooler increases, each TE cooler compensates a higher fraction of the estimated cooling load. This

behavior occurs because the resulting thermal resistance of the heat sink rapidly decreases with the number of thermocouples per TE cooler (see Fig. 5(f)). The present behavior of the thermal resistance of the heat sink is examined next.

From Eq. (5), the thermal resistance of the heat sink, R_{hs}, is the sum of the fin resistance, R_f, and the base spreading resistance, R_b. According to Eq. (6), the fin resistance depends on the geometric parameters and the material properties of the heat sink. The latter are assumed to remain constant in this study. All the geometric parameters of the heat sink (i.e. L_f, W_f, t_f, n_f, and t_b) are made design variables in the optimization formulation. The results from Table 2 indicate that the heat sink design converges to the same optimal geometry for all the configurations. Hence, the values of the fin resistance, R_f, are equal for all design configurations evaluated in this study.

However, the base spreading resistance, R_b, of the heat sink behaves differently. As the number of thermocouples per TE cooler increases, the area of the TE cooler, A_{sc}, also increases [14]. Since the optimal geometry of the heat sink is independent of the TE cooler configuration, the base area of the heat sink, A_b, is constant for all the design configurations evaluated in this study, and is equal to $A_b = (2n_f - 1)t_f w_f = 4950\ \text{mm}^2$. For a constant base area, the base spreading resistance, R_b, of the heat sink decreases as the TE cooler area increases (Eq. (11)). Fig. 5(g) shows the base spreading resistance for each design configuration evaluated in this study. We observe that the base spreading resistance decreases rapidly as the number of thermocouples per TE cooler increases (Fig. 5(g)). Because of this decrease in the base spreading resistance, the total heat sink resistance, R_{hs}, decreases as the number of thermocouples per TE cooler increases (Fig. 5(f)), and is not constant—as was the fin resistance R_f.

As stated in Section 2.2, the primary requirement of a heat sink is to provide a low thermal resistance path for heat dissipation. From Fig. 5(f), the design configurations with 127 thermocouples per TE cooler have heat sinks with the least thermal resistance. However, this observation does not imply that these configurations have superior heat dissipation capabilities. In the *thermal circuit* of the TE unit, the heat sinks are parallel to each other. The thermal resistance of the complete TE unit, R_{th}^{TE}, is determined by dividing the thermal resistance of a single heat sink, R_{hs}, by the number of heat sinks, N. The thermal resistances of the TE units are shown in Table 2. We can observe that the design configurations with seven thermocouples per TE cooler results in the lowest R_{th}^{TE} values, and those with 127 thermocouples per TE cooler results in the highest R_{th}^{TE} values, for all of the values of λ. We can also observe that the thermal resistance of the TE unit decreases with the number of thermocouples per TE cooler.

However, it is important to note that through the optimization process, appropriate heat sinks have been designed for all the TE unit configurations to dissipate the entire heat generated at the hot junction of the TE coolers (Q_{ph}). Interestingly, the thermal resistance of the heat sink is not the primary criterion for selecting the TE unit configuration for the generic enclosure.

5.8. Hot side temperature

We conclude this section by explaining how the hot side temperature of the TE cooler is not a significant driving factor in the selection of the TE coolers configuration.

Fig. 5(h) depicts the hot side temperature of the TE cooler (T_h) for each of the design configurations. The hot side temperature is plotted against the number of thermocouples per TE cooler. We observe that the hot side temperature increases with the number of thermocouples per TE cooler. In the previous section we noted that each TE cooler compensates a higher fraction of the cooling load as the number of thermocouples per TE cooler increases. This situation leads to an accompanying increase in the hot side temperature of the TE cooler. Appropriate heat sinks are then designed to dissipate the required heat. Further, the hot side temperature of the TE cooler is much lower than the maximum allowable temperature, T_{max} [14]. Hence, the hot side temperature of the TE cooler is not likely to be the primary criterion for selecting the appropriate design configuration of the TE unit.

6. Conclusions

A multi-objective optimization based design strategy was proposed to design the thermoelectric unit (TE unit) of ABE systems. The application of the proposed design strategy was demonstrated by designing a TE unit for a generic enclosure. Computationally favorable approximate analytical models of the TE cooler and heat sink were developed for a preliminary optimization study. The cooling load was estimated for a generic enclosure. The developed optimization approach was implemented to evaluate 18 different design configurations of the TE unit. The results indicate that the total input power required to operate the TE unit decreases as the distribution density of the TE coolers increases. It was observed that the thermal resistance of the heat sink plays a key role in determining the optimal number of TE coolers in all of the design configurations. Based on the assumptions made in the study, the TE unit configuration involving 20 TE coolers of CP1.0-17-05L type was found to be optimal for the generic enclosure. This design represents a trade-off between the input power requirement

and the number of TE coolers used in the TE unit. However, the multi-objective nature of the formulation allows the incorporation of different designer preferences with respect to these objectives. This paper represents the first step in the development of a design and analysis approach for the practical implementation of ABE systems.

Acknowledgements

Support from the National Science Foundation, award number CMS—0333568, Directorate for Engineering, Division of Civil and Mechanical Systems, and the US Department for Housing and Urban Development is much appreciated.

References

[1] S. Van Dessel, A. Messac, R. Khire, Active building envelopes: a preliminary analysis, in: Asia International Renewable Energy Conference, Beijing, China, 2004.
[2] D.D. Pollock, Thermocouples: Theory and Practice, CRC Press Inc., Boca Raton, FL, 1991, ISBN 0-8493-4243-0.
[3] A.F. Ioffe, Semiconductor Thermoelements and Thermoelectric Cooling, Infosearch Limited, London, 1957.
[4] D.M. Rowe, CRC Handbook of Thermoelectrics, IEEE, CRC Press, 1995, ISBN 0-8493-0146-7.
[5] J.R. Baird, D.F. Fletcher, B.S. Haynes, Local condensation heat transfer rates in fine passages, Int. J. Heat Mass Transfer 46 (23) (2003) 4453–4466.
[6] W. Seifert, M. Ueltzen, E. Muller, One-dimensional modeling of thermoelectric cooling, Phys. Stat. Sol. (a) 194 (1) (2002) 277–290.
[7] J.P. Holman, Heat Transfer, fifth ed., McGraw-Hill Inc., USA, 1981, ISBN 0-07-0296189.
[8] S. Lee, Calculating spreading resistance in heat sinks, Electron. Cooling 4 (1) (1998) 30–33.
[9] Enertron Inc., Optimization of heat sink design and fan selection in portable electronics environment, Research Article available on the official website of Enertron Inc., April 2004.
[10] M.J. Nagy, R. Buist, Effect of heat sink design on thermoelectric cooling performance, AIP Conf. Proc. 316 (1) (1994) 147–149.
[11] J.A. Visser, D.J. de Kock, Optimization of heat sink mass using the DYNAMIC-Q numerical optimization method, Commun. Numer. Methods Eng. 18 (10) (2002) 721–727.
[12] R. Khire, S. Van Dessel, A. Messac, Active building envelopes: a new solar driven heat transfer mechanism, in: 19th European PV Solar Energy Conference, Paris, France, 2004.
[13] A. Messac, A. Ismail-Yahaya, Required relationship between objective function and Pareto frontier orders: Practical implications, AIAA J. 39 (11) (2001) 2168–2174.
[14] Melcor Corporation, Melcor Thermal Solutions Catalog, 2004, pp. 47–49. Available from: <www.melcor.com>.
[15] M.A. Green, Solar Cells: Operating Principles, Technology, and System Application, Prentice-Hall, Inc., Englewood Cliff, NJ, 1982, ISBN 0-13-822270-3.